Interplay between electric and magnetic effect in adiabatic polaritonic systems

Alessandro Alabastri,[1] Andrea Toma,[1] Carlo Liberale,[1] Manohar Chirumamilla,[1] Andrea Giugni,[1] Francesco De Angelis,[1] Gobind Das,[1] Enzo Di Fabrizio,[1,2,3] and Remo Proietti Zaccaria[1,*]

[1]*Istituto Italiano di Tecnologia (IIT), via Morego 30, 16163 Genova, Italy*
[2]*BIONEM Laboratory, University of Magna Graecia, Campus S. Venuta, Germaneto, viale Europa, I88100 Catanzaro, Italy*
[3]*King Abdullah University of Science and Technology (KAUST), Thuwal 23955, Saudi Arabia*
[*]*remo.proietti@iit.it*

Abstract: We report on the possibility of realizing adiabatic compression of polaritonic wave on a metallic conical nano-structure through an oscillating electric potential (quasi dynamic regime). By comparing this result with an electromagnetic wave excitation, we were able to relate the classical lighting-rod effect to adiabatic compression. Furthermore, we show that while the magnetic contribution plays a marginal role in the formation of adiabatic compression, it provides a blue shift in the spectral region. In particular, magnetic permeability can be used as a free parameter for tuning the polaritonic resonances. The peculiar form of adiabatic compression is instead dictated by both the source and the metal permittivity. The analysis is performed by starting from a simple electrostatic system to end with the complete electromagnetic one through intermediate situations such as the quasi-electrostatic and quasi-dynamic regimes. Each configuration is defined by a particular set of equations which allows to clearly determine the individual role played by the electric and magnetic contribution in the generation of adiabatic compression. We notice that these findings can be applied for the realization of a THz nano-metric generator.

© 2013 Optical Society of America

OCIS codes: (240.6680) Surface Plasmons; (240.5420) Polaritons; (250.5403) Plasmonics; (260.3910) Metal optics.

References and links

1. M. I. Stockman, "Nanofocusing of optical energy in tapered plasmonic waveguides," Phys. Rev. Lett. **93,** 137404 (2004).
2. J. D. Jackson, *Classical Electrodynamics* (John Wiley & Sons, 1998).
3. J. A. H. van Nieuwstadt, M. Sandtke, R. H. Harmsen, F. B. Segerink, J. C. Prangsma, S. Enoch, L. Kuipers, "Strong modification of the nonlinear optical response of metallic subwavelength hole arrays," Phys. Rev. Lett. **97,** 146102 (2006).
4. A. Belardini, M. C. Larciprete, M. Centini, E. Fazio, C. Sibilia, M. Bertolotti, A. Toma, D. Chiappe, F. Buatier de Mongeot, "Tailored second harmonic generation from self-organized metal nano-wires arrays," Opt. Express **17,** 3603–3609 (2009).
5. J. K. Gansel, M. Thiel, M. S. Rill, M. Decker, K. Bade, V. Saile, G. von Freymann, S. Linden, M. Wegener, "Gold helix photonic metamaterials as broadband circular polarizer," Science **325,** 1513–1515 (2009).
6. J. Song, R. Proietti Zaccaria, G. Dong, E. Di Fabrizio, M. B. Yu, and G. Q. Lo, "Evolution of modes in a metal-coated nano-fiber," Opt. Express **19,** 25206–25221 (2011).

#183313 - $15.00 USD Received 10 Jan 2013; revised 28 Feb 2013; accepted 1 Mar 2013; published 19 Mar 2013

7. A. Belardini, M. C. Larciprete, M. Centini, E. Fazio, C. Sibilia, D. Chiappe, C. Martella, A. Toma, M. Giordano, F. Buatier de Mongeot, "Circular dichroism in the optical second-harmonic emission of curved gold metal nanowires," Phys. Rev. Lett. **107,** 257401 (2011).
8. L. Razzari, A. Toma, M. Shalaby, M. Clerici, R. Proietti Zaccaria, C. Liberale, S. Marras, I.A.I. Al-Naib, G. Das, F. De Angelis, M. Peccianti, A. Falqui, T. Ozaki, R. Morandotti and E. Di Fabrizio, "Extremely large extinction efficiency and field enhancement in terahertz resonant dipole nanoantennas," Opt. Express **19,** 26088–26094 (2011).
9. F. De Angelis, F. Gentile, F. Mecarini, G. Das, M. Moretti, P. Candeloro, M. L. Coluccio, G. Cojoc, A. Accardo, C. Liberale, R. Proietti Zaccaria, G. Perozziello, L. Tirinato, A. Toma, G. Cuda, R. Cingolani, and E. Di Fabrizio, "Breaking the diffusion limit with super-hydrophobic delivery of molecules to plasmonic nanofocusing SERS structures ," Nat. Photon. **5,** 682–687 (2011).
10. S. V. Boriskina and M. R. Bjorn, "Molding the flow of light on the nanoscale: from vortex nanogears to phase-operated plasmonic machinery," Nanoscale **4,** 76–90 (2012).
11. N. A. Janunts, K. S. Baghdasaryan, Kh. V. Nerkararyan, and B. Hecht, "Excitation and superfocusing of surface plasmon polaritons on a silver-coated optical fiber tip," Opt. Commun. **253,** 118–124 (2005).
12. P. Corio, S. D.M. Brown, A. Marucci, M. A. Pimenta, K. Kneipp, G. Dresselhaus, and M. S. Dresselhaus, "Surface-enhanced resonant Raman spectroscopy of single-wall carbon nanotubes adsorbed on silver and gold surfaces," Phys. Rev. B **61,** 13202–13211 (2000).
13. F. De Angelis, M. Patrini, G. Das, I. Maksymov, M. Galli, L. Businaro, L. C. Andreani, and E. Di Fabrizio, "A hybrid plasmonic-photonic nanodevice for label-free detection of a few molecules," Nano Lett. **8,** 2321–2327 (2008).
14. W. Zhang, X. Cui, and O. J. F. Martin, "Local field enhancement of an infinite conical metal tip illuminated by a focused beam," J. Raman Spectrosc. **40,** 1338–1342 (2009).
15. T. J. Davis, D. E. Gomez, and K. C. Vernon, "Evanescent coupling between a Raman-active molecule and surface plasmons in ensembles of metallic nanoparticles," Phys. Rev. B **82,** 205434 (2010).
16. F. De Angelis, G. Das, P. Candeloro, M. Patrini, M. Galli, A. Bek, M. Lazzarino, I. Maksymov, C. Liberale, L. C. Andreani, and E. Di Fabrizio, "Nanoscale chemical mapping using three-dimensional adiabatic compression of surface plasmon polaritons," Nat. Nanotech. **5,** 67–72 (2010).
17. P. I. Geshev, U. Fischer, and H. Fuchs, "Calculation of tip enhanced Raman scattering caused by nanoparticle plasmons acting on a molecule placed near a metallic film," Phys. Rev. B **81,** 125441 (2010).
18. B. Fazio, C. D'Andrea, F. Bonaccorso, A. Irrera, G. Calogero, C. Vasi, P. G. Gucciardi, M. Allegrini, A. Toma, D. Chiappe, C. Martella, F. Buatier de Mongeot, "Re-radiation enhancement in polarized surface-enhanced resonant raman scattering of randomly oriented molecules on self-organized gold nanowires," ACS Nano **5,** 5945–5956 (2011).
19. M. I. Haftel, C. Schlockermann and G. Blumberg, "Role of cylindrical surface plasmons in enhanced transmission," Appl. Phys. Lett. **88,** 193104 (2006).
20. L. Novotny, "Effective wavelength scaling for optical antennas," Phys. Rev. Lett. **98,** 266802 (2007).
21. T. Sondergaard and S. Bozhevolnyi, "Slow-plasmon resonant nanostructures: scattering and field enhancements," Phys. Rev. B **75,** 073402 (2007).
22. E. J. Smythe, E. Cubukcu and F. Capasso, "Optical properties of surface plasmon resonances of coupled metallic nanorods," Opt. Express **15,** 7439–7447 (2007).
23. G. W. Bryant, F. J. Garca de Abajo and J. Aizpurua, "Mapping the plasmon resonances of metallic nanoantennas," Nano Lett. **8,** 631–636 (2008).
24. E. S. Barnard, J. S. White, A. Chandran and M. L. Brongersma, "Spectral properties of plasmonic resonator antennas," Opt. Express **16,** 16529–16537 (2008).
25. A. J. Babadjanyan, N. L. Margaryan, and Kh. V. Nerkararyan, "Superfocusing of surface polaritons in the conical structure ," J. Appl. Phys. **87,** 3785–3788 (2000).
26. R. Ruppin, "Effect of non-locality on nanofocusing of surface plasmon field intensity in a conical tip," Phys. Lett. A **340,** 299–302 (2005).
27. L. Vaccaro, L. Aeschimann, U. Staufer, H. P. Herzig, and R. Dandliker, "Propagation of the electromagnetic field in fully coated near-field optical probes ," Appl. Phys. Lett. **83,** 584–586 (2003).
28. W. Ding, S. R. Andrews, and S. A. Maier, "Internal excitation and superfocusing of surface plasmon polaritons on a silver-coated optical fiber tip," Phys. Rev. A **75,** 063822 (2007).
29. C. C. Neacsu, S. Bergewer, R. L. Olmon, L. V. Saraf, C. Ropers, and M. B. Raschke, "Near-field localization in plasmonic superfocusing: a nanoemitter on a tip," Nano Lett. **10,** 592–596 (2010).
30. D. K. Gramotnev, M. W. Vogel, and M. I. Stockman, "Optimized nonadiabatic nanofocusing of plasmons by tapered metal rods," J. Appl. Phys. **104,** 034311 (2008).
31. J. S. Lee, S. Han, J. Shirdel, S. Koo, D. Sadiq, C. Lienau, and N. Park, "Superfocusing of electric or magnetic fields using conical metal tips: effect of mode symmetry on the plasmon excitation method," Opt. Express **19,** 12342–12347 (2011).
32. R. Proietti Zaccaria, A. Alabastri, F. De Angelis, G. Das, C. Liberale, A. Toma, A. Giugni, L. Razzari, M. Malerba, H. B. Sun, and E. Di Fabrizio, "Fully analytical description of adiabatic compression in dissipative

#183313 - $15.00 USD Received 10 Jan 2013; revised 28 Feb 2013; accepted 1 Mar 2013; published 19 Mar 2013
(C) 2013 OSA

polaritonic structures," Phys. Rev. B **86,** 035410 (2012).
33. A. D. Rakic, A. B. Djuriic, J.M. Elazar, and M. L. Majewski, "Optical properties of metallic films for vertical-cavity optoelectronic devices," Appl. Opt. **37,** 5271–5283 (1998).
34. S. A. Mayer, *Plasmonics: Fundamentals and Applications* (Springer, 2007).
35. D. Sarid and W. Challener, *Modern introduction to Surface Plasmons* (Cambridge University Press, 2010).
36. The Drude-Lorentz model is a commonly adopted method to describe the interaction between a metallic medium and an electromagnetic field. The model itself does not require the definition of any wave vector $\vec{k}$, but it just assumes the presence of an oscillating electric field. Ought to this aspect, we will exploit the Drude-Lorentz model in all our numerical analysis except the ES case.
37. P. A. Belov, R. Marques, S. I. Maslovski, I. S. Nefedov, M. Silveirinha, C. R. Simovski, and S. A. Tretyakov, "Strong spatial dispersion in wire media in the very large wavelength limit," Phys. Rev. B **67,** 113103 (2003).
38. K. B. Crozier, A. Sundaramurthy, G. S. Kino, and C. F. Quate, "Optical antennas: resonator for local field enhancement," J. Appl. Phys. **94**, 4632 (2003).
39. C. Huang, X. Yin, H. Huang and Y. Zhu, "Study of plasmon resonance in a gold nanorod with an LC circuit model," Opt. Express **17,** 6407–6413 (2009).
40. F. De Angelis, R. Proietti Zaccaria, M. Francardi, C. Liberale, and E. Di Fabrizio, "Multi-scheme approach for efficient surface plasmon polariton generation in metallic conical tips on AFM-based cantilevers," Opt. Express **19,** 22268–22279 (2011).
41. R. Proietti Zaccaria, F. De Angelis, A. Toma, L. Razzari, A. Alabastri, G. Das, C. Liberale, and E. Di Fabrizio, "Surface plasmon polariton compression through radially and linearly polarized source," Opt. Lett. **37,** 545–547 (2012).
42. M. I. Stockman, "Nanoplasmonics: past, present, and glimpse into future," Opt. Express **19,** 22029–22106 (2011).
43. S. Linden, C. Enkrich, G. Dolling, M. W. Klein, J. Zhou, T. Koschny, C. M. Soukoulis, S. Burger, F. Schmidt, and M. Wegener, "Photonic metamaterials: magnetism at optical frequencies," IEEE J. Sel. Top. Quantum Electron. **12**, 1097–1105 (2006).
44. J. Zhou, T. Koschny, M. Kafesaki, E. N. Economou, J. B. Pendry, and C. M. Soukoulis, "Saturation of the magnetic response of split-ring resonators at optical frequencies," Phys. Rev. Lett. **95,** 223902 (2005).
45. P. Bharadwaj, A. Bouhelier, and L. Novotny, "Electrical excitation of surface plasmons," Phys. Rev. Lett. **106,** 226802 (2011).

1. Introduction

Adiabatic compression is the phenomenon describing the increase of the electric field associated to a reduction of both the phase and group velocity of a polaritonic wave when it approaches the tip-end of a metallic conical structure [1]. The electrostatic counterpart of this phenomenon, the lighting rod effect, takes its physical origin from the equipotential condition of a conductor surface and thus charge densities need to grow more in tapered regions generating high electric fields in the surrounding medium [2]. High intensity electric field in a small region of space becomes crucial to trigger several physical phenomena [3–11] and it can be exploited for the design of Raman sensor-based applications [12–18] which may consider elongated nanosized structures [19–24]. Surface Plasmon Polaritons (SPPs) have been utilized as a mechanism to concentrate energy in small regions [1, 25–30] and to spatially separate the far-field source from the excited region [31, 32]. In particular, high signal-to-noise ratio can be achieved when metallic conical nano-devices exploit adiabatic compression. Here we explain the role of electrostatic (constant electric potential, ES), quasi-electrostatic (slowly -few THz- oscillating electric potential, QES) and quasi-dynamic (oscillating electric potential, QD) electric fields in the realization of resonances on nano-sized metallic conical structures, and we compare their effects with the electromagnetic (EM) case which has been proved to create adiabatic compression [1]. We will demonstrate that this optical phenomenon can be obtained also under QD conditions, whose limit to low frequency is represented by the QES condition (ES for zero frequency). In particular, we will show the relation between the two phenomena lighting-rod effect and adiabatic compression. Furthermore, we will extrapolate the main cause of adiabatic compression: electric field distribution and permittivity. In fact, we will show that the magnetic contribution does not play any role in the formation of adiabatic compression [31], however it is responsible for the resonance position in the spectral range. This characteristics

#183313 - $15.00 USD Received 10 Jan 2013; revised 28 Feb 2013; accepted 1 Mar 2013; published 19 Mar 2013
(C) 2013 OSA

can play an interesting role for engineering polaritonic resonances of metallic nano-cones in QD regime. To be noted that for all the four cases, the frequency range is below the plasma frequency of the conical metallic structure (for silver, $\omega_p = 2172$ THz ~ 138 *nm* [33]).

2. Theoretical background

Plasmons are collective electronic oscillations which can be induced in metallic-like dispersive materials. Depending on the type of excitation, coupling conditions and geometry we can refer either to bulk plasmons, surface plasmons (SPs) or localized plasmons (LPs). In particular, bulk plasmons are longitudinal oscillations triggerable at the plasma frequency of the bulk material, which for noble metals usually lies in the UV region (e.g., the plasma wavelength of gold is 137.5 *nm*). However, since the transverse characteristic of electromagnetic waves, bulk plasmons cannot be optically excited [34]. SPs are electromagnetic waves propagating along the interface between a dielectric and a conductor, evanescently decaying in both media. They can be optically excited provided that the source is TM polarized and under proper coupling conditions which guarantee the conservation of both the energy and the wave vector. Finally, LPs are non-propagating waves which can be induced in metallic nanostructures. In particular, they are characterized by the oscillation of surface electrons which are resonant at certain frequencies, hence leading to an electric near-field enhancement.

For simple geometries such as nano-spheres, the resonant condition can be retrieved analytically by solving the Mie scattering problem [2]. When are instead considered more elongated and complex geometries such as cylinders or cones, the problem of finding the resonant conditions can have different approaches. In these cases, SPs and LPs can be correlated: in fact LPs can be seen as the final results of SPs propagating back and forth along the structure while experiencing self interference. For example, Barnard *et al*. in [24] show how a Fabry-Prot resonator model can predict resonances in nano-strip antennas. In the particular case of a conical structure, SPs properties do not depend solely on the source frequency which intrinsically sets the value of the dispersive medium dielectric permittivity. In fact, the SPs propagation is correlated to the effective refractive index of the structure which, for a tapered geometry, is coordinate dependent. Considering a surface plasmon propagating from the base of a nano-cone up to its apex, its associated wavelength would undergo a progressive shrinking ought to the increase of the effective refractive index of the medium which, in turn, is associated to the decreasing of the section of the cone [35]. This results implies a decreasing of the wave group velocity, namely SPs progressively slow down and concentrate in a narrow region where the electric field may be enhanced even of some orders of magnitude. Overall, this process can be termed as adiabatic compression.

3. Modeling

We start by considering a silver cone interacting with a plane wave linearly polarized along the cone axis with an electric field amplitude of 1 V/m. All the calculations were performed by using either *Comsol Multiphysics* package or *Mathematica* software. Comsol is a simulation software based on finite element analysis; the minimum mesh size for the electromagnetic simulations was set to 1 *nm* to reproduce the apex features of the conical structure. Given the geometry of the problem (inset in Fig. 1) we expect the electrons in the metal to oscillate mainly in the *z* direction. In such circumstances their motion strongly depends on the frequency of the incident wave. The parameter which describes the medium optical response is the permittivity which can be expressed, according to the Drude-Lorentz model, with a combination of oscilla-

#183313 - $15.00 USD Received 10 Jan 2013; revised 28 Feb 2013; accepted 1 Mar 2013; published 19 Mar 2013
(C) 2013 OSA

tors [33]:

$$\varepsilon_r = 1 - \frac{\Omega_p^2}{\omega(\omega - i\Gamma_0)} + \sum_{j=1}^{m} \frac{f_j \omega_p^2}{(\omega_j^2 - \omega^2) + i\omega\Gamma_j} \tag{1}$$

where ω_p is the metal plasma frequency, m stands for the number of oscillators with lifetime $1/\Gamma_j$, strength f_j and frequency ω_j. $\Omega_p = \sqrt{f_0}\omega_p$ is the modified plasma frequency that includes the oscillator strength f_0. It should be noted that ε_r can be written in terms of the complex conductivity $\sigma(\omega)$, namely $\varepsilon_r = 1 + \sigma(\omega)/i\omega\varepsilon_0$, expression which will return useful in the discussion of the QD case [36]. Finally, in the present theory, no spatial dispersion was taken into account [26, 37].

In Fig. 1 it is shown the norm of the electric field $|E| = (E_x^2 + E_y^2 + E_z^2)^{1/2}$ for a wide range of frequencies (from 4 THz to 600 THz or 75 μm to 500 *nm*). The cone is 2.5 μm long with 150 *nm* base radius. The tip-end is defined by a 5 *nm* radius of curvature. The values are taken on the cone axis 5 *nm* off its apex when the plane wave is traveling in the *x* direction. We chose to evaluate the field intensity in this position since it is close to the sharp tip-end where we expect the free charges of the metal to accumulate [38]. We notice the first peak at around 51 THz (5878 *nm*). Increasing the frequency several other peaks occur, corresponding to higher order resonances. This behavior is similar to the response of a metallic cylinder with the main difference in the node distribution [20]. In fact, while in a cylinder the inter-node distance is constant, in a cone, ought to its geometrical properties, the inter-node distance tends to shrink

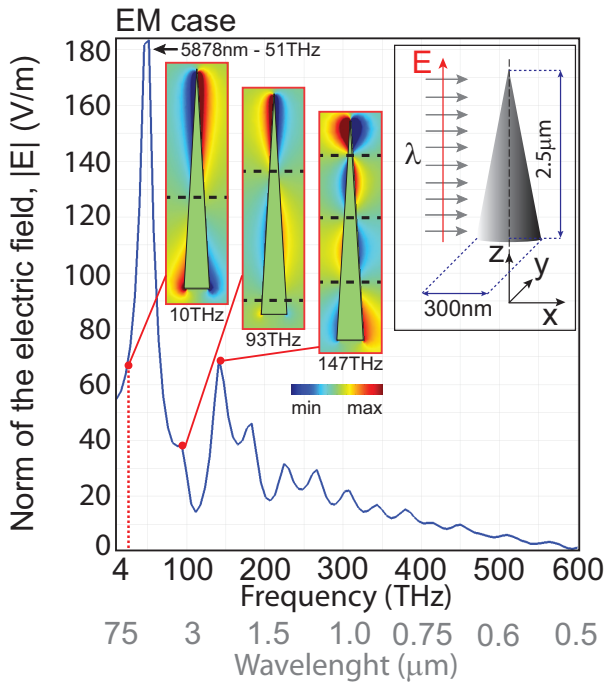

Fig. 1. Spectrum of the norm of the electric field calculated on the cone axis 5 *nm* off the tip-end. The strongest peak, corresponding to the fundamental dipole mode, is found at 5878 *nm* ($\sim$ 51 THz). No peaks are found for lower frequencies. The figure shows also the sketch of the the illumination method together with the x-component of the electric field for three frequencies: 10 THz, 93 THz and 147 THz. For each of them the nodal planes are indicated by dashed lines.

#183313 - $15.00 USD Received 10 Jan 2013; revised 28 Feb 2013; accepted 1 Mar 2013; published 19 Mar 2013
(C) 2013 OSA

approaching the tip apex. Furthermore, an overall shift of the nodes toward the tip apex is observed by increasing the excitation frequency. In particular, in the IR/visible range, these features are known to be related to the generation of SPPs on the cone surface which undergo adiabatic compression. The position of the resonances is dependent on both the aspect ratio [39] of the cone and on the apex angle. The three mode profiles in Fig. 1 confirm the previous description. For completeness, it should be noted that when moving from any dip in the electric field profile to the next peak at higher frequency (positive derivative of the norm of the electric field), only a slight shift of the existent nodes toward the tip apex is observed, however no new nodes appear in the mode distribution. For example, when moving from the mode distribution at 10 THz to 51 THz (not shown), only a slight shift in the position of the single node toward the tip apex is observed.

4. ES, QES, EM: a face to face comparison

At very low frequency, such as 10 THz (30 μm), the source wavelength is much bigger than the dimensions of the cone, which allows the use of the quasi-static approximation, where the device does not experience any retardation effect [35]. Therefore, low-frequency (QES) and static (ES) regimes are expected to converge in terms of charges response and corresponding electric field. Figure 2 shows the profile of the electric field norm calculated on a line along the

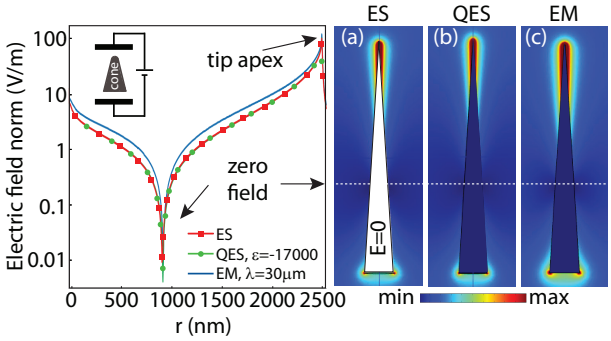

Fig. 2. E-field norm calculated along a line from the base to the apex of the cone. The line is 1 *nm* above the cone surface (in the dielectric). Three situations are considered: (a) equipotential condition on the cone is assumed (ES case); (b) slowly oscillating field (10 THz) characterized by strongly negative permittivity $\varepsilon = -17000$ (QES case); (c) electromagnetic source with $\lambda = 30\ \mu m$ (EM case). For the three cases the field amplitude is set at 1 V/m. A common zero is found at ~ 950 *nm* from the base. (a), (b) and (c) are the corresponding E-field plots on the *xz* plane.

cone surface and extending from its base ($r = 0$ *nm*) to the apex ($r \sim 2500$ *nm*). The calculation was performed for three different situations: (a) the cone is inserted inside a capacitor whose plates are perpendicular to the cone axis (see sketch in Fig. 2). The applied potential is set such that the static electric field between the plates is fixed at 1 V/m. It is assumed to have the cone in equipotential state, namely the oscillation frequency of the field is set equal to zero (ES case); (b) same configuration as in (a) with the assumption of a slowly oscillating electric field. The oscillating frequency of the capacitor is chosen to be 10 THz which corresponds to a strongly negative permittivity $\varepsilon = -17000$ for the silver (QES); (c) an electromagnetic radiation with $\lambda = 30\ \mu m$ (red dotted line in Fig. 1) impinges on the cone along x direction. The field amplitude is 1 V/m (EM case). The results demonstrate that for all three configurations the electric field norms show the same behavior: the field undergoes a local enhancement ought to the sharp edges at the cone basis, reaches a zero at around 950 *nm* from the base, grows up to its

#183313 - $15.00 USD Received 10 Jan 2013; revised 28 Feb 2013; accepted 1 Mar 2013; published 19 Mar 2013
(C) 2013 OSA

maximum at the tip end and, finally, it sharply decreases just outside the metal. This description is confirmed by the plots in Figs. 2(a)-2(c) where dipole-like field patterns calculated in the *xz* plane passing through the axis of the cone are shown. As foreseen, the field patterns in the three cases are the same with the only difference that the case (a) does not show any field inside the metal ought to the equipotential assumption.

We shall now specify what was calculated in the three previously considered cases. In both the *ES* and *QES* cases (Figs. 2(a) and 2(b), respectively), electrostatic equations (no magnetic contribution) are solved:

$$\begin{cases} \vec{D} = \varepsilon_0 \varepsilon_r \vec{E} \\ \nabla \cdot \vec{D} = \rho \\ \vec{E} = -\nabla V \end{cases} \tag{2}$$

In particular, for the ES case, the electric permittivity ε is calculated only for the surrounding medium (sm) while the cone is set in equipotential state. On the other hand, for the QES case, the quantity ε is defined for the complete simulation domain (cone and surrounding medium). In fact, even though permittivities are derived to describe the interaction between matter and EM waves (which includes both the electric and magnetic contributions) through the Drude-Lorentz model, a low frequency wave is physically similar to a static electric field by simply taking a very low negative value for the cone permittivity (at $\omega = 10$ THz, $\varepsilon = -17000$). As we have seen, this work-around gives reliable results (Fig. 2(b)), even though it is not as physically rigorous as the ES case. Finally, for the *EM case* (Fig. 2(c)), the Helmholtz equation is solved:

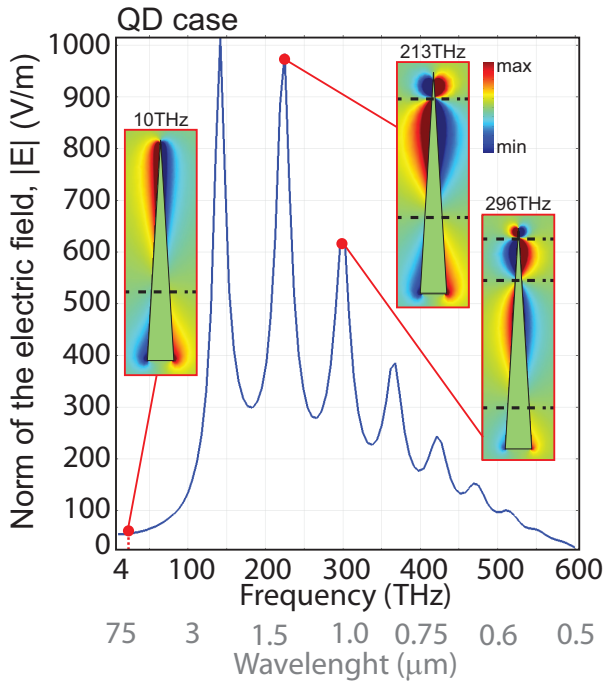

Fig. 3. Spectrum of the norm of the electric field calculated at 5 *nm* from the tip-apex for the QD case. Strong blue-shift is found with respect to the EM case (Fig. 1). The first three mode profiles for the x-component of the electric field are also shown. The dashed lines represent the nodal planes.

$$\nabla \times \mu_r^{-1} (\nabla \times \vec{E}) - k_0^2 \varepsilon_r \vec{E} = 0 \tag{3}$$

#183313 - $15.00 USD Received 10 Jan 2013; revised 28 Feb 2013; accepted 1 Mar 2013; published 19 Mar 2013
(C) 2013 OSA

where the relative magnetic permeability μ_r has been set to 1 both for the cone and for the surrounding medium.

5. The QD approximation

The next step is to consider an electric potential *oscillating* between the capacitor plates (QD case). Differently by the QES case, no slowly oscillating field assumption is made, however, similarly to the QES case, no magnetic contributions are considered ($\mu_{cone} = \mu_{sm} \equiv 0$). In this situation the calculated equations include the possibility of electric currents:

$$\begin{cases} \vec{D} = \varepsilon_0 \varepsilon_r \vec{E} \\ \nabla \cdot \vec{D} = \rho \\ \vec{E} = -\nabla V \\ \nabla \cdot \vec{J} + \frac{\partial \rho}{\partial t} = 0 \\ \vec{J} = i\omega \vec{D} = \sigma(\omega) E + \varepsilon_0 \frac{\partial E}{\partial t} \end{cases} \tag{4}$$

Figure 3 shows the electric field dependence from the source wavelength for the QD case. As in Fig. 1, the field is calculated 5 *nm* off the tip-end along the cone axis. Interestingly, the spectrum shows a behavior recalling the trend of Fig. 1, with a number of resonant peaks all associated to a specific light mode. In particular, the insets in the figure are associated to three different modes calculated at 10 THz, 213 THz (second peak) and 296 THz (third peak). Clearly, by increasing the frequency, the number of nodes in the field amplitude goes from one to three. This is the same behavior seen in Fig. 1. However, a blue-shift exists between the two spectra. In fact, the fundamental mode for the QD case is centered around 150 THz, hence about 100 THz blue-shifted with respect to the EM case (51 THz). Furthermore, the electric field for the QD configuration results to be roughly one order of magnitude higher than in the corresponding EM case. We anticipate that this effect can be explained in terms of magnetic field contribution. Indeed, for the QD case, only the electric field contribution was considered.

6. QD vs. EM

Turning again our attention toward the EM case, it has been proved the possibility to create SPPs along a metallic cone also by means of linearly polarized light [40, 41]. Figure 4 compares the electric field distribution for the seventh resonant peak of the EM (315 THz) and QD (528 THz) cases. This peak was chosen inasmuch it shows a sufficient number of nodal planes to qualitatively represent the adiabatic compression. Interestingly, not only EM but also the QD case shows the typical adiabatic compression behavior. In fact, as previously suggested, the magnetic field plays little role in the definition of the polaritonic field, hence adiabatic compression is shown also by the QD case. This result agrees with the electromechanical definition of plasmonic energy [42]. The frequency shift between the 7^{th} peak in the EM and QD cases is consequence of the different permeability μ. In fact, while the QD case is defined by $\mu = 0$, the EM case in Fig. 1 is characterized by $\mu_{sm} = \mu_{cone} = 1$. Figure 5 shows the existence of saturation frequencies, characteristic already described for metallic nanostructures in relation with the size scalability [39, 43, 44]. This phenomenon basically sets a limit in the use of plasmonic structures and metamaterials in the optical range. Here we find that the same saturation can also be directly related to the media magnetic response. In the zero limit of both μ_{sm} and μ_{cone}, the EM frequency would overlap the QD case, as shown in Fig. 5. Obviously the counter behavior is also expected: the inclusion of the magnetic contribute into the QD case would return a response equal to the EM case. In Fig. 5 are also shown the resonance shifts when only μ_{sm} is changed, while $\mu_{cone} = 1$. Clearly, a blue-shift is observed by decreasing μ_{sm}. Many interesting points can be explained by looking at both Fig. 4 and Fig. 5. First of all, an increase

#183313 - $15.00 USD Received 10 Jan 2013; revised 28 Feb 2013; accepted 1 Mar 2013; published 19 Mar 2013
(C) 2013 OSA

of the frequency leads to a decrease of the field amplitude. This is explained by the dipole response shown by the mode at the tip apex. In fact, it can be demonstrated that the electric field generated by a dipole shows an amplitude decrease by increasing the frequency. Furthermore, choosing a specific resonance, the QD case shows a field amplitude much higher than the EM case. Figure 5 demonstrates how this behavior is related to the value of the magnetic permeability. In fact, a decrease of the relative permeability leads to an increase of the field amplitude. This response is explained by considering the simple model of an oscillating electric dipole: i) the relation between the electric field E and both the electric scalar potential V and the magnetic vector potential $\vec{A}$; ii) the magnetic vector potential for an oscillating dipole:

$$\begin{cases} \vec{E} = -\vec{\nabla}V - \frac{\partial \vec{A}}{\partial t} \\ \vec{A} = \frac{\mu}{4\pi}\frac{\dot{\vec{p}}}{r} \end{cases} \tag{5}$$

where r is the spatial coordinate and $\vec{p}$ is the dipole momentum. By solving the system, it is found that for metallic structures an increase of μ implies a decrease of the electric field.

Finally, in Fig. 4 we also observe different positions for the nodal planes of the electric field between QD and EM case. In particular, the EM case shows zeros shifted toward the cone base.

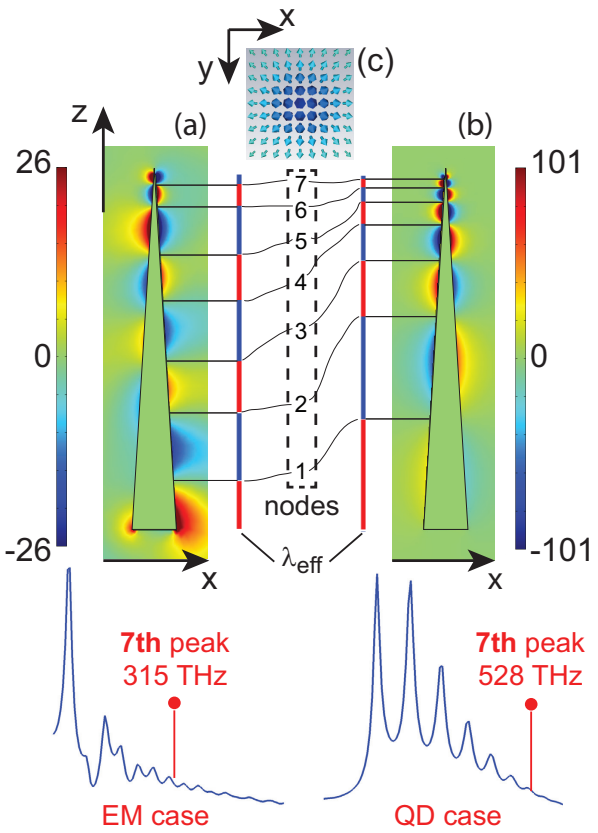

Fig. 4. x-component of the electric field for a) EM case; b) QD case. For both cases the seventh order peak was considered, corresponding to 315 THz and 528 THz for EM and QD case, respectively (see bottom plots, Fig. 1 (left) and 3 (right)). Adiabatic compression (shrinkage of λ_{eff}) is clearly shown through the red/blue scale indicating the nodes positions. c) Radial mode calculated 5 *nm* off the cone apex.

#183313 - $15.00 USD Received 10 Jan 2013; revised 28 Feb 2013; accepted 1 Mar 2013; published 19 Mar 2013
(C) 2013 OSA

This is related to the previous arguments of lower field for higher μ. In fact, considering the overall power conservation, at lower field values must be associated higher effective wavelength λ_{eff} hence determining a node shift toward the tip base for the EM case when compared to the QD case.

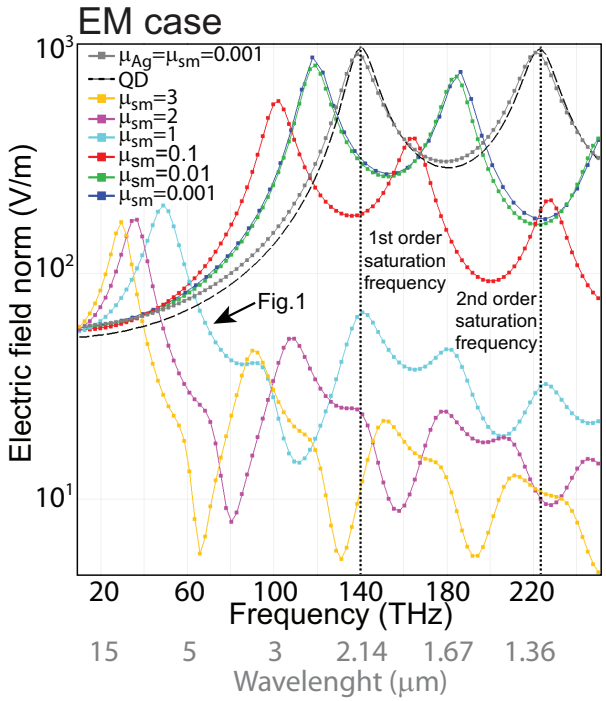

Fig. 5. Norm of the electric field calculated at 5 *nm* off the tip apex by changing the relative magnetic permeability μ_{sm} ($\mu_{cone} = 1$ unless otherwise specified). The curve with $\mu_{sm} = 1$ corresponds to Fig. 1. By decreasing μ_{sm} a blue-shift is observed. The QD case is also plotted for comparison with the EM zero limit of both μ_{sm} and μ_{cone} resulting in a overlapping of the two curves. The first two saturation frequency orders are shown by the two vertical dotted lines. The ordinate is in log scale.

These observations can now be exploited in order to relate the lighting rod effect and adiabatic compression. In fact, while the former is usually associated to the ES case (or QD at low frequencies), the latter is historically associated to a EM radiation in the visible/IR range. In reality, as seen in Fig. 4 and Fig. 5, this division is purely arbitrary. Both phenomena can be shown by QD and EM case, depending on the frequency (i.e., $\omega \to 0$: lighting rod effect; $\omega > 0$: adiabatic compression).

7. Conclusion

In conclusion, we have studied the interaction of static, quasi-static, quasi-dynamics and electromagnetic fields with a metallic silver nano-structure with the purpose of investigating the generation of adiabatic compression. It was found that adiabatic compression does not strictly require any electromagnetic radiation to be generated, in fact also quasi-dynamics fields can provide an adiabatic compression behavior. This result can lead to a future development of highly efficient energy concentrators, such as metallic conical tips, working on electrical excitation (for example by means of tunneling electrons [45]) instead of laser systems. In fact, we

#183313 - $15.00 USD Received 10 Jan 2013; revised 28 Feb 2013; accepted 1 Mar 2013; published 19 Mar 2013
(C) 2013 OSA

have demonstrated that only the electric contribution is responsible for adiabatic compression, while the magnetic part is associated to both the resonance position and the field intensity. This last aspect might be considered for tuning the resonance of conical structures by acting on the magnetic permeability μ.

Acknowledgments

The authors gratefully acknowledge support from European Projects Nanoantenna FP7-HEALTH-2009, Grant No. 241818 and FOCUS FP7 No. 270483.

#183313 - $15.00 USD Received 10 Jan 2013; revised 28 Feb 2013; accepted 1 Mar 2013; published 19 Mar 2013
(C) 2013 OSA